

# Journal of Biomedical Optics

BiomedicalOptics.SPIEDigitalLibrary.org

## **Biodegradable microsphere-mediated cell perforation in microfluidic channel using femtosecond laser**

Atsuhiko Ishii  
Kazumasa Ariyasu  
Tatsuki Mitsuhashi  
Dag Heinemann  
Alexander Heisterkamp  
Mitsuhiro Terakawa

**SPIE.**

Atsuhiko Ishii, Kazumasa Ariyasu, Tatsuki Mitsuhashi, Dag Heinemann, Alexander Heisterkamp, Mitsuhiro Terakawa, "Biodegradable microsphere-mediated cell perforation in microfluidic channel using femtosecond laser," *J. Biomed. Opt.* **21**(5), 055001 (2016), doi: 10.1117/1.JBO.21.5.055001.

# Biodegradable microsphere-mediated cell perforation in microfluidic channel using femtosecond laser

Atsuhiko Ishii,<sup>a</sup> Kazumasa Ariyasu,<sup>a</sup> Tatsuki Mitsuhashi,<sup>a</sup> Dag Heinemann,<sup>b</sup> Alexander Heisterkamp,<sup>b,c</sup> and Mitsuhiro Terakawa<sup>a,\*</sup>

<sup>a</sup>Keio University, Department of Electronics and Electrical Engineering, 3-14-1 Hiyoshi, Kohoku-ku, Yokohama 223-8522, Japan

<sup>b</sup>Laser Zentrum Hannover e.V., Biomedical Optics Department, Hollerithallee 8, Hannover D- 30419, Germany

<sup>c</sup>Gottfried Wilhelm Leibniz University Hannover, Institute of Quantum Optics, Am Welfengarten 1, Hannover 30167, Germany

**Abstract.** The use of small particles has expanded the capability of ultrashort pulsed laser optoinjection technology toward simultaneous treatment of multiple cells. The microfluidic platform is one of the attractive systems that has obtained synergy with laser-based technology for cell manipulation, including optoinjection. We have demonstrated the delivery of molecules into suspended-flowing cells in a microfluidic channel by using biodegradable polymer microspheres and a near-infrared femtosecond laser pulse. The use of polylactic-co-glycolic acid microspheres realized not only a higher optoinjection ratio compared to that with polylactic acid microspheres but also avoids optical damage to the microfluidic chip, which is attributable to its higher optical intensity enhancement at the localized spot under a microsphere. Interestingly, optoinjection ratios to nucleus showed a difference for adhered cells and suspended cells. The use of biodegradable polymer microspheres provides high throughput optoinjection; i.e., multiple cells can be treated in a short time, which is promising for various applications in cell analysis, drug delivery, and *ex vivo* gene transfection to bone marrow cells and stem cells without concerns about residual microspheres. © 2016 Society of Photo-Optical Instrumentation Engineers (SPIE) [DOI: 10.1117/1.JBO.21.5.055001]

Keywords: femtosecond laser; laser cell perforation; optoinjection; microfluidics; biodegradable polymer.

Paper 160041R received Jan. 22, 2016; accepted for publication Apr. 18, 2016; published online May 9, 2016.

## 1 Introduction

Ultrashort pulsed lasers play a growing role in biology and medicine as a tool for precise ablation of cell organelles and cell membranes.<sup>1-5</sup> Cell membrane perforation by focused femtosecond laser pulses provides an exclusive technology to introduce external molecules into a single cell, i.e., optoinjection, without significant cell damage because of a nonlinear interaction in a tiny focused spot.<sup>6-9</sup> Recently, the use of nanoparticles or microparticles has been accelerating attractive achievements to expand the capability of ultrashort laser optoinjection technology toward simultaneous treatment of multiple cells. Chakravarty et al.<sup>10</sup> reported the delivery of DNA, protein, and fluorescence molecules into cells in a cuvette by using carbon black nanoparticles and a femtosecond laser. Another promising method is the use of gold nanoparticles, which has been called gold nanoparticles-mediated (GNOME) laser transfection.<sup>11-15</sup> Boulais et al.<sup>15,16</sup> stated that the generation of shock waves in water by the interaction of gold nanoparticles and ultrashort laser pulses is attributable to plasma expansion mediated by plasmonic near-field instead for rapid temperature increase. The scheme for GNOME laser transfection shows applications for cell manipulation reported in the latest publications.<sup>17,18</sup>

The microfluidic platform is one of the attractive systems for obtaining synergy with laser-based technology for cell manipulation, including optoinjection. Microfluidic chips have been used for dispensing,<sup>19</sup> cell analyzing,<sup>20</sup> and cell sorting<sup>21</sup> as

well as drug delivery.<sup>22,23</sup> In 2010, Marchington et al.<sup>24</sup> reported automated optoinjection into cells by using a microfluidic chip fabricated in polydimethylsiloxane. Propidium iodide was used for the evaluation of molecular uptake. Optoinjection by using a femtosecond Bessel beam was applied as well with the objective of higher throughput, which was reported by the same group.<sup>25</sup> The throughput rate of cell treatment and the optoinjection ratio were 10 cells/s and 20.4%, respectively. Transfection of plasmid DNA was demonstrated by using a cell-flow system and focused femtosecond laser pulses in 2014.<sup>26</sup> Similar to conventional optoinjection, the use of particles enables treatment of multiple cells in a microfluidic chip. Lukianova-Hleb et al.<sup>27</sup> demonstrated cell-selective optical injection in a flow system by using 60-nm diameter gold nanoparticles and picosecond laser pulses. Despite the fact that the throughput of optical injection with particles is higher than that found with only a focused laser scheme, a limited number of papers have reported optical injection with the use of particles in microfluidic chips.

In this study, we demonstrated the delivery of molecules into suspended-flowing cells in a microfluidic channel by using biodegradable polymer microspheres and a near-infrared femtosecond laser pulse. The method is based on our previous studies on biodegradable microsphere-mediated cell membrane perforation.<sup>28-30</sup> Polylactic acid (PLA) microspheres and polylactic-co-glycolic acid (PLGA) microspheres are compared for optoinjection to flow cells, followed by the discussion of the delivery of molecules to nucleus, based on the comparison with optoinjection to adhered cells.

\*Address all correspondence to: Mitsuhiro Terakawa, E-mail: [terakawa@elec.keio.ac.jp](mailto:terakawa@elec.keio.ac.jp)

## 2 Materials and Methods

### 2.1 Cell Culture and Microsphere Conjugation

Human epithelial carcinoma cells (A431 cells) were used in this study. The cells were cultured in Dulbecco's modified Eagle medium supplemented with 10% fetal bovine serum (Thermo Fisher Scientific, Waltham, Massachusetts) under a humidified atmosphere of 95% air and 5% CO<sub>2</sub> at 37°C. The cells were harvested and seeded as a monolayer in culture dishes for the experiments. Optoinjection experiments were performed for cells at ~80% confluency. Cells were trypsinized at the confluency after microsphere conjugation for experiments using microfluidic chips.

PLA microspheres and PLGA microspheres of 2 μm in diameter were used in this study. PLA and PLGA are U. S. Food and Drug Administration-approved biodegradable polymers that have been widely used in clinical practice. The surface of the microspheres was modified with protein A to bind antiepidermal growth factor receptor mouse monoclonal antibody (clone 528, Thermo Fisher Scientific, Waltham, Massachusetts). The mixture of the microspheres and the antibody was stirred for 25 min at room temperature, then unbound antibody was removed by centrifugation for 10 min at 10,000 rpm. The bound microspheres were resuspended in phosphate-buffered saline (PBS) and added to A431 cells for conjugation. After 40 min, unbound microspheres were washed out by PBS. The number of microspheres bound to a single cell is <10, confirmed by optical microscope observation (Fig. 1).

### 2.2 Microfluidic Chip and Optical Injection

The linear microchannel was fabricated on fused silica, which was covered by welded cover glass (0.5-mm thickness) on top. The length, width, and depth of the channel were 50.8 mm, 300 μm, and 100 μm, respectively. Figure 2 shows a schematic (a) and a photograph (b) of the microfluidic chip. Tubes were connected with lure lock connectors to both ends of the channels. Microsphere-conjugated cells were trypsinized and flowed through the channel with fluorescein isothiocyanate (FITC)-dextran (2 MDa and 2 μM). The diameters of detached cells

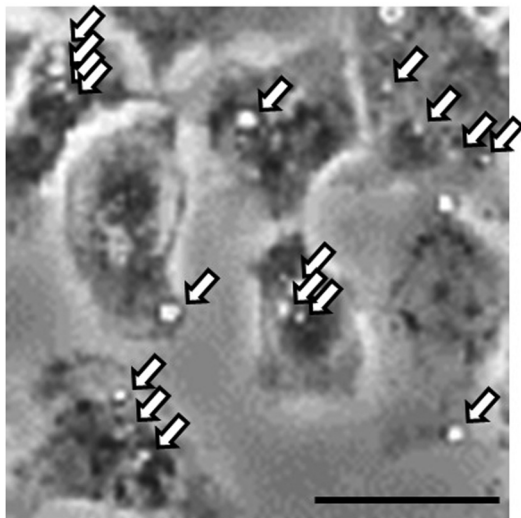


**Fig. 1** Phase contrast image of A431 cells after the conjugation of PLGA microspheres. Microspheres are indicated with arrows. Scale bar indicates 30 μm.

flowing in the channel were ~30 μm. The flow rate was controlled by a syringe driver, which was kept to 32.4 ml/h, corresponding to the flow speed of 300 μm/ms in the channel. The cell concentration was  $1.3 \times 10^4$  cells/ml; therefore, the treatment throughput was ~110 cells/s. Cells were collected on the other end of the channel, and FITC-dextran, which was not uptaken by the cells, was removed by centrifuge. Fluorescent molecules uptaken by the cells were observed by using a fluorescence microscope (Eclipse Ti-E, Nikon, Tokyo, Japan) 24 h after the laser illumination. The cell viability was evaluated by trypan blue dye-exclusion test. Optoinjection to adhered cells was also investigated for comparison. The detailed protocol for adhered cells is the same as that we have described in our previous papers.<sup>29,30</sup>

A Ti:sapphire chirped pulse amplification laser system (Libra, Coherent, Santa Clara, California), which generates 80-fs laser pulses at an 800-nm central wavelength, was used. The repetition rate of the laser was 1 kHz. The linearly polarized laser pulse was weakly focused on the microfluidic channel by using a plano-convex lens ( $f = 200$  mm) to a laser spot size of 300 μm. The flow speed of cells in the channel was 300 μm/ms, as described above. The cells were presumed to be illuminated by a single shot of laser pulse from the top side of the channel. No adhesion of a cell to the surface of the channel was observed after the flow with laser illumination.

The experiments were performed for five samples in each experimental condition. The optoinjection ratio was determined by the number of cells showing fluorescence to the total number of cells counted, expressed as means ± standard error. The fluorescence intensity was evaluated and the threshold of the intensity was settled to determine the fluorescent cells. The average number of cells counted was 80 for each condition. Statistical analysis was performed on the basis of the nonparametric Mann–Whitney test. A value of  $p < 0.01$  was considered statistically significant.

### 2.3 Finite Difference Time Domain

We performed the numerical analysis of optical field distributions by three-dimensional (3-D) finite difference time domain (FDTD) simulation. The simulation model consisted of a single PLA ( $n = 1.45$ ) or PLGA ( $n = 1.60$ ) microsphere of 2 μm in diameter in water ( $n = 1.33$ ). The plane wave at the wavelength of 800 nm was incident from the top of a microsphere at the normal incidence. The incident wave was linearly polarized along the  $x$ -axis.

## 3 Results

Figure 3 shows the dependence of the optoinjection ratio to cells in microfluidic channel on laser fluence. The optoinjection ratio at 0.7 J/cm<sup>2</sup>, which is the highest laser fluence we have used for flowing cells, is ~10% using PLA microspheres. The ratio at 0.7 J/cm<sup>2</sup> with PLA microspheres is comparable to that for adhered cells, which was described in our previous study using PLA microspheres.<sup>30</sup> The ratio increased at fluences higher than 0.8 J/cm<sup>2</sup> in the case of adhered cells in the previous paper; however, the highest laser fluence we have used for suspended-flowing cells in the present study was 0.7 J/cm<sup>2</sup> to avoid modification or damage in the fused silica chip under the microchannel by self-focusing of the laser pulse. For an alternative solution to increase the optoinjection ratio, we have used PLGA microspheres. The optoinjection ratio with PLGA microspheres showed higher values compared to that

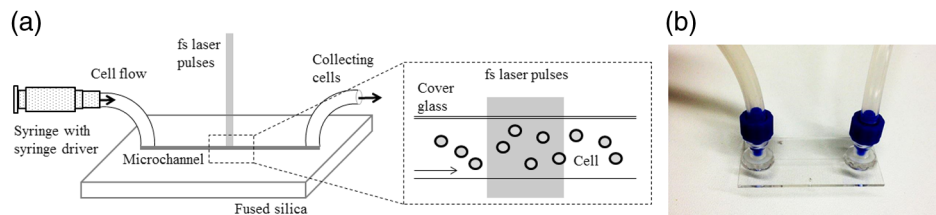
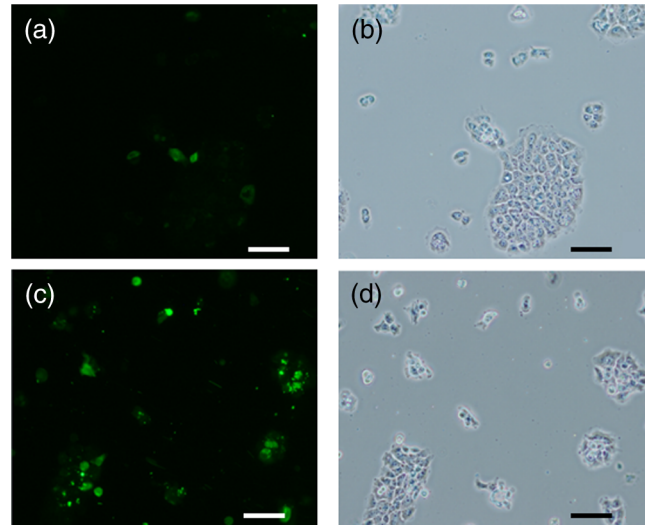


**Fig. 2** (a) Schematic diagram and (b) a photograph of the microfluidic chip for optoinjection using a femtosecond laser pulse and biodegradable microspheres. A linearly shaped microchannel (length 50.8 mm, width  $300\ \mu\text{m}$ , and depth  $100\ \mu\text{m}$ ) was fabricated on fused silica, which was covered by welded cover glass (0.5-mm thickness) on top.

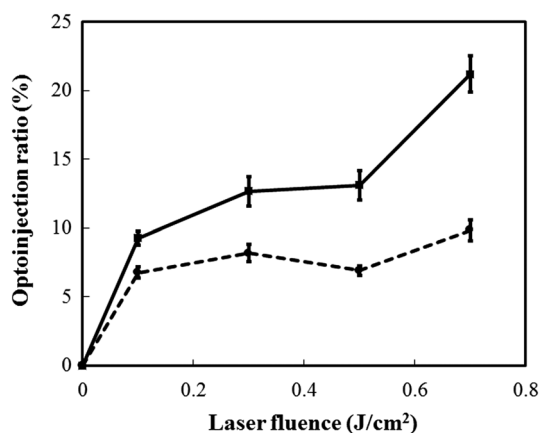
with PLA microspheres. The ratio reached more than 20% at  $0.7\ \text{J}/\text{cm}^2$  using PLGA microspheres, which is a comparable percentage to that of adhered cells at laser fluences higher than  $1.0\ \text{J}/\text{cm}^2$ .<sup>30</sup> No optoinjected cell was observed without laser illumination. Additionally, no optoinjected cell was observed without microspheres even at a laser fluence of  $0.7\ \text{J}/\text{cm}^2$ , which was highest laser fluence in this study. The survival rates were higher than 95% at all conditions for flowing cells in the experiments.

Figure 4 shows fluorescence images (a and c) and phase contrast images (b and d) of the cells 24 h after laser illumination. Because fluorescence molecules that were not uptaken by cells were washed out carefully, unperforated cells show no fluorescence. Cell aggregations that can be seen in the images probably occurred in procedures after the flow through the microchannel. Interestingly, the fluorescence in cells shows different distributions depending on the cells. Some cells show fluorescence in cytoplasm but low fluorescence in the nucleus. The distribution is likely to be independent from fluorescence intensity.

We have evaluated the distribution of fluorescence molecules in cells based on the presence of fluorescence in the nucleus. Figures 5(a) and 5(b) represent the cells showing fluorescence in the nucleus and those showing low fluorescence intensity in the nucleus, respectively, after optoinjection using PLGA microspheres. The ratios of cells that showed fluorescence in the cytoplasm only and those that showed it in the nucleus to the total number of cells counted are shown in Fig. 5(c). In addition, the ratio of cells showing fluorescence in the nucleus to the total



**Fig. 4** (a and c) Fluorescence images and (b and d) phase contrast images of A431 cells 24 h after laser illumination. The cells were perforated using PLGA microspheres illuminated by femtosecond laser pulse in the presence of 2 MDa FITC-dextran. The laser fluences were (a and b)  $0.1\ \text{J}/\text{cm}^2$  and (c and d)  $0.7\ \text{J}/\text{cm}^2$ . Scale bars =  $100\ \mu\text{m}$ .



**Fig. 3** Dependence of optoinjection ratio of 2 MDa FITC-dextran to flow cells on the laser fluence. PLA microspheres (dashed line) and PLGA microspheres (solid line) were used to interact with the femtosecond laser pulse. The experiments were performed for five samples in each condition ( $n = 5$ ). Error bars represent the error of the mean.

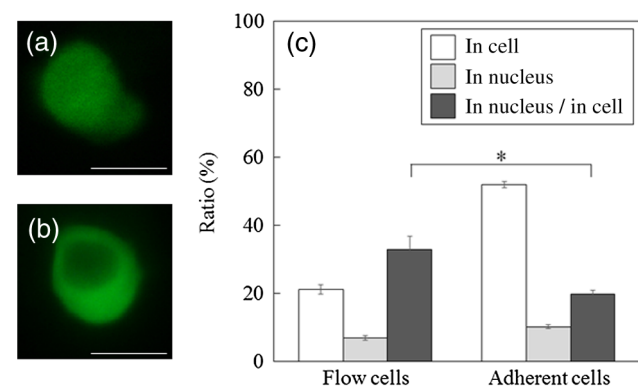


**Fig. 5** Typical cell showing (a) fluorescence in nucleus and (b) low fluorescence intensity in nucleus after optoinjection using PLGA microspheres. Scalebars =  $20\ \mu\text{m}$ . (c) The optoinjection ratios into cells (white bars) and into nucleus (gray bars). The ratios of optoinjection into the nucleus to the total number of optoinjected cells are also shown (black bars). The experiments were performed for five samples in each condition ( $n = 5$ ) at the laser fluence of  $0.7\ \text{J}/\text{cm}^2$  for flow cells and adherent cells. Error bars represent the error of the mean ( $*p < 0.01$ ).



number of optoinjected cells is shown. The ratios for adhered cells using PLGA microspheres are also shown for comparison. The optoinjection ratio, i.e., cells showing fluorescence in cytoplasm, is higher for adhered cells; however, it should be noted that the ratio of cells that show fluorescence in the nucleus to the total number of optoinjected cells is higher for flow cells using the microfluidic channel. Although we have not used a confocal microscope, this result shows a certain degree of evaluation in the difference of distribution of molecules. The ratio of cells showing fluorescence in the nucleus to optoinjected cells is 32.9% for flow cells at laser fluence of  $0.7 \text{ J/cm}^2$ , which is statistically significantly higher than that obtained for adhered cells at the same laser fluence (19.7%). The ratio of optoinjected cells in the case of adhered cells in the present study is higher than what we reported in the previous paper with PLA.<sup>30</sup> This is attributable to the difference in microsphere materials.

#### 4 Discussion

Optoinjection in a microfluidic platform requires consideration of laser energy, especially for the case of ultrashort laser pulses. High-peak intensity of the femtosecond laser could lead to self-focusing, multiphoton absorption, and, possibly, optical breakdown<sup>31,32</sup> in the fused silica chip located under the microfluidic channel, which could cause damage and change in the optical properties of the chip material. In the present study, we used a  $100\text{-}\mu\text{m}$  depth microchannel fabricated on a fused silica chip of  $1.0\text{-mm}$  thickness. The propagating length of a femtosecond laser pulse in fused silica after optoinjection is  $0.9 \text{ mm}$ , which is much thicker than the case of our previous study using a glass-bottomed cultured dish whose thickness was  $80$  to  $120 \mu\text{m}$ . Therefore, lower peak intensity is desirable for developing the microfluidic laser perforation system. We used PLGA for an alternative microsphere to PLA to obtain higher optical peak intensity at the focused optical field under microspheres without increasing incident laser energy. Figure 6 shows optical field distributions around a PLA microsphere (a) and a PLGA microsphere (b) calculated by 3-D FDTD simulation. A microsphere works as a microlens, and the optical intensity under the sphere is enhanced compared to incident optical intensity.<sup>33</sup> The microspheres conjugated to the top side of the cell at the laser illumination contributed to cell membrane perforation. The microspheres conjugated to the side

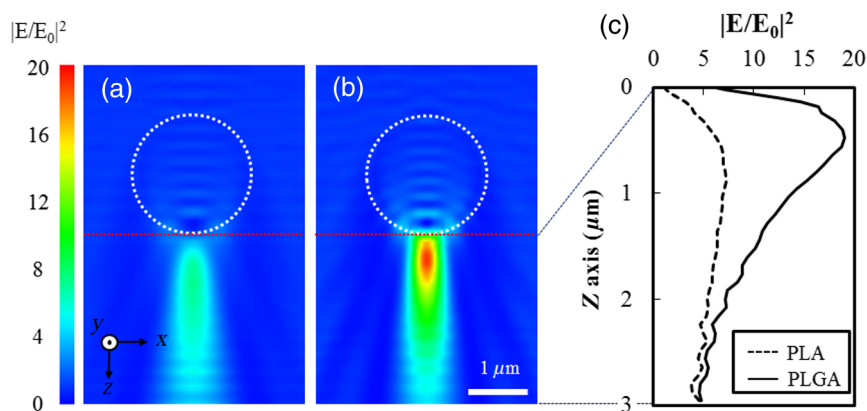


**Fig. 6** Optical field distributions on the  $xz$  plane simulated by the 3-D FDTD method for (a) PLA microspheres and (b) PLGA microspheres of  $2\text{-}\mu\text{m}$  diameter. A plane wave is illuminated to the microspheres with the wave vector in the  $z$ -direction. The incident wave is linearly polarized along the  $x$ -axis and is  $800 \text{ nm}$  in wavelength. (c) Optical intensity enhancement with PLA microspheres (dashed line) and with PLGA microspheres (solid line) along the  $z$ -axis under the spheres.

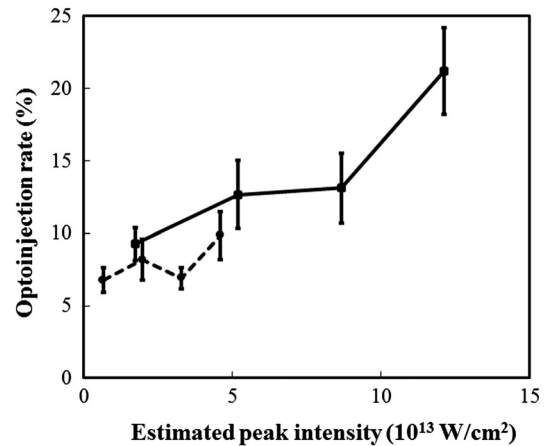


**Fig. 7** Dependence of optoinjection ratio on estimated optical peak intensity PLA microspheres (dashed line) and PLGA microspheres (solid line) derived from Figs. 3 and 6(c). Error bars represent the error of the mean.

surface or the opposite side of the laser illumination may contribute less to direct interaction, but possibly affect adjacent cells or have a localized shock wave-mediated effect. The simulation results clearly show that the peak optical intensity under PLGA microspheres is higher than that with PLA microspheres. The higher optoinjection ratios achieved by using PLGA compared to those using PLA shown in Fig. 3 are attributable to the difference in the optical intensity enhancements by PLGA and PLA, in which the peak optical intensity under PLGA microspheres is 2.6 times higher than that with PLA microspheres. Figure 7 shows the dependence of the optoinjection ratio on estimated peak intensity under the microspheres derived from Figs. 3 and 6. Because the enhancement factor by PLGA is higher than that by PLA, the peak intensities are calculated to be higher for PLGA. Note that the optoinjection ratios are comparable for PLA and PLGA when normalized by peak intensity under the microspheres, which supports our discussion in a previous study that the perforation mechanism is governed by the optical intensity under the microspheres in the case of biodegradable microsphere-mediated laser perforation.<sup>29</sup> These results show not only the higher optoinjection ratio we can obtain with PLGA, but also

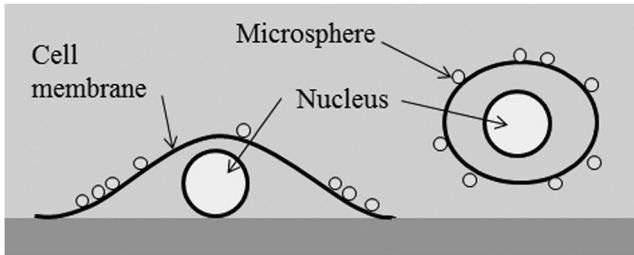


**Fig. 8** Illustration of the relative positions of cells and microspheres for an adhered cell and a flow cell.

a practical advantage that PLGA microspheres enable us to use lower incident laser energy to the microfluidic chip, resulting in the prevention of optical damage to the chip.

The ratio of cells showing fluorescence in the nucleus to optoinjected cells is higher for flow cells compared to adhered cells [Fig. 5(c)]. One of the possible explanations for the delivery to the nucleus is the difference in the relative position of a cell and conjugated microspheres, as shown in Fig. 8. Unlike the enhanced plasmonic optical field with metallic particles, the focused intensity lasts for a distance of a few micrometers along the  $z$ -axis under the microsphere (Fig. 6). In the case of flow cells, cells are spherical in shape when they flow in the microchannel. Biodegradable microspheres are dispersively conjugated to the entire surface of a cell with a certain randomness, while adhered cells have microspheres on the top side. Microspheres conjugated to the laser-illuminated side could contribute to cell membrane perforation. The enhanced optical zone could interact with the nuclear membrane if the microsphere is located on the cell membrane above the nucleus. In this case, the nuclear delivery is dependent on the probability of the presence of microspheres above the nucleus. In case of adhered cells, however, the distribution of biodegradable microspheres is inhomogeneous. This was demonstrated by the phase contrast image of the adhered A431 cells after the microsphere conjugation in Fig. 1 as well as a figure in our previous paper.<sup>29</sup> Most of the microspheres were conjugated to the shallow slope of the cell surface, and only a few microspheres can be seen on the top of a cell lifted by the presence of a nucleus. Enhanced optical fields generated under microspheres on the shallow slope could interact with cell membranes, but not with nuclear membranes.

One of the advantages of particle-mediated optoinjection is higher throughput treatment of cells compared to a method using a focused femtosecond laser, which treats cells one by one. The first paper on optoinjection in microfluidic chips using focused femtosecond laser pulses reported the treatment rate of a single cell per second.<sup>24</sup> The throughput of this method has improved to 10 cells/s by changing cell velocity as well as the use of Bessel beam, reported by Rendall et al.<sup>25</sup> Because cells flow any place in a microfluidic channel, beam targeting of flow cells in a microchannel is one of the key challenges to achieving successful optoinjection. Rendall et al. achieved hydrodynamic focusing by using a 3-D nozzle and confined cells in the central region of the microchannel. As another approach, Breunig et al.<sup>26</sup> improved the cell treatment ratio by an axially elongated laser focus region and line scanning perpendicular to the flow direction. It is obvious that a wide channel would be suitable not only because of the increased number of cells flowing simultaneously, but also to avoid cells becoming stuck in a narrow channel. Although the

treatment of individual cells is not easy in optoinjection by using microspheres with an unfocused/weakly focused beam, throughput is higher because all cells flowing in the microchannel can be treated regardless of the flowing region in the microfluidic channel. Although the treatment rate was 110 cells/s in the present study, further increase could easily be achieved by increasing the density of flow cells and widening the microfluidic channel. The use of PLGA microspheres contributes to an increase the number of cells treatable per second with the same output power of a laser by beam expansion because of its higher enhancement factor of optical intensity under the microspheres.

## 5 Conclusion

In this study, we have demonstrated optoinjection of flow cells in a microfluidic channel by using a femtosecond laser and biodegradable polymer microspheres. FDTD simulation shows the result that PLGA microspheres generate a higher enhancement factor of optical intensity under microspheres compared to that with PLA microspheres. This enhancement contributed to obtaining not only a higher optoinjection ratio but also avoiding damage to the microfluidic chip. Optoinjection ratios to nucleus showed a difference for adhered cells and flow cells. Further discussion is necessary, but one of the possible explanations is the relative position of microspheres on the cell. The utilization of biodegradable polymer microspheres provides higher throughput optoinjection; i.e., multiple cells can be treated in a short time, which is promising for various applications in cell analysis, drug delivery, and *ex vivo* gene transfection to bone marrow cells and stem cells without concerns about residual microspheres.

## Acknowledgments

This work was supported in part by the JSPS KAKENHI for Challenging Exploratory Research, Grant No. 26560263.

## References

1. K. König et al., "Intracellular nanosurgery with near infrared femtosecond laser pulses," *Cell. Mol. Biol.* **45**(2), 195–201 (1999).
2. U. K. Tirlapur and K. König, "Targeted transfection by femtosecond laser," *Nature* **418**, 290–291 (2002).
3. S. H. Chung and E. Mazur, "Surgical applications of femtosecond lasers," *J. Biophotonics* **2**(10), 557–572 (2009).
4. S. K. Gokce et al., "A fully automated microfluidic femtosecond laser axotomy platform for nerve regeneration studies in *C. elegans*," *PLoS One* **9**(12), e113917 (2014).
5. T. Higaki et al., "Statistical organelle dissection of Arabidopsis guard cells using image database LIPS," *Sci. Rep.* **2**, 405 (2012).
6. A. A. Davis et al., "Optoporation and genetic manipulation of cells using femtosecond laser pulses," *Biophys. J.* **105**(4), 862–871 (2013).
7. C. A. Mitchell et al., "Femtosecond optoinjection of intact tobacco BY-2 cells using a reconfigurable photoporation platform," *PLoS One* **8**(11), e79235 (2013).
8. K. Dhakal, B. Black, and S. Mohanty, "Introduction of impermeable actin-staining molecules to mammalian cells by optoporation," *Sci. Rep.* **4**, 6553 (2014).
9. M. Antkowiak et al., "Femtosecond optical transfection of individual mammalian cells," *Nat. Protoc.* **8**, 1216–1233 (2013).
10. P. Chakravarty et al., "Delivery of molecules into cells using carbon nanoparticles activated by femtosecond laser pulses," *Nat. Nanotechnol.* **5**(8), 607–611 (2010).
11. M. Schomaker et al., "Plasmonic perforation of living cells using ultrashort laser pulses and gold nanoparticles," *Proc. SPIE* **7192**, 71920U (2009).

12. D. Heinemann et al., "Gold nanoparticle mediated laser transfection for efficient siRNA mediated gene knock down," *PLoS One* **8**(3), e58604 (2013).
13. S. Kalies et al., "Enhancement of extracellular molecule uptake in plasmonic laser perforation," *J. Biophotonics* **7**(7), 474–482 (2014).
14. J. Baumgart et al., "Off-resonance plasmonic enhanced femtosecond laser optoporation and transfection of cancer cells," *Biomaterials* **33**(7), 2345–2350 (2012).
15. E. Boulais et al., "Plasmonics for pulsed-laser cell nanosurgery: fundamentals and applications," *J. Photochem. Photobiol. C* **17**, 26–49 (2013).
16. E. Boulais, R. Lachaine, and M. Meunier, "Plasma-mediated nanocavitation and photothermal effects in ultrafast laser irradiation of gold nanorods in water," *J. Phys. Chem. C* **117**(18), 9386–9396 (2013).
17. S. Kalies et al., "Investigation of biophysical mechanisms in gold nanoparticle mediated laser manipulation of cells using a multimodal holographic and fluorescence imaging setup," *PLoS One* **10**(4), e0124052 (2015).
18. S. Kalies et al., "Characterization of the cellular response triggered by gold nanoparticle-mediated laser manipulation," *J. Biomed. Opt.* **20**(11), 115005 (2015).
19. M. J. Ahamed et al., "A piezoactuated droplet-dispensing microfluidic chip," *J. Microelectromech. Syst.* **19**(1), 110–119 (2010).
20. V. Lecaute et al., "Microfluidic single cell analysis: from promise to practice," *Curr. Opin. Chem. Biol.* **16**(3–4), 381–390 (2012).
21. T.-H. Wu et al., "Pulsed laser triggered high speed microfluidic fluorescence activated cell sorter," *Lab Chip* **12**(7), 1378–1383 (2012).
22. N. Nguyen et al., "Design, fabrication and characterization of drug delivery systems based on lab-on-a-chip technology," *Adv. Drug Delivery Rev.* **65**(11–12), 1403–1419 (2013).
23. N. Huang et al., "Recent advancements in optofluidics-based single-cell analysis: optical on-chip cellular manipulation, treatment, and property detection," *Lab Chip* **14**(7), 1230–1245 (2014).
24. R. F. Marchington et al., "Optical injection of mammalian cells using a microfluidic platform," *Biomed. Opt. Exp.* **1**(2), 527–536 (2010).
25. H. A. Rendall et al., "High-throughput optical injection of mammalian cells using a Bessel light beam," *Lab Chip* **12**(22), 4816–4820 (2012).
26. H. G. Breunig et al., "High-throughput continuous flow femtosecond laser-assisted cell optoporation and transfection," *Microsc. Res. Tech.* **77**(12), 974–979 (2014).
27. E. Y. Lukianova-Hleb et al., "Cell-specific transmembrane injection of molecular cargo with gold nanoparticle-generated transient plasmonic nanobubbles," *Biomaterials* **33**(21), 5441–5450 (2012).
28. M. Terakawa and Y. Tanaka, "Dielectric microsphere mediated transfection using femtosecond laser," *Opt. Lett.* **36**(15), 2877–2879 (2011).
29. M. Terakawa, Y. Tsunoi, and T. Mitsuhashi, "In vitro perforation of human epithelial carcinoma cell with antibody-conjugated biodegradable microspheres illuminated by a single 80 fs near-infrared laser pulse," *Int. J. Nanomed.* **7**, 2653–2660 (2012).
30. T. Mitsuhashi and M. Terakawa, "Evaluation of parameters influencing the molecular delivery by biodegradable microsphere-mediated perforation using femtosecond laser," *J. Biomed. Opt.* **19**(1), 015003 (2014).
31. K. Sugioka and Y. Cheng, "Ultrafast lasers—reliable tools for advanced materials processing," *Light Sci. Appl.* **3**, e149 (2014).
32. C. B. Shaffer, A. Brodeur, and E. Mazur, "Laser-induced breakdown and damage in bulk transparent materials induced by tightly focused femtosecond laser pulses," *Meas. Sci. Technol.* **12**(11), 1784–1794 (2001).
33. M. Terakawa et al., "Enhanced localized near field and scattered far field for surface nanophotonics applications," *Prog. Quantum Electron.* **36**(1), 194–271 (2012).

**Atsuhiko Ishii** is a graduate school student at Keio University, Japan. He received his BS degree in electronics and electrical engineering from Keio University. His research interests include mechanism and applications of laser cell perforation.

**Kazumasa Ariyasu** received his BS and MS degrees from Keio University in 2014 and 2016, respectively. His research interests include laser-based drug delivery and drug release.

**Tatsuki Mitsuhashi** received his BS and MS degrees from Keio University in 2012 and 2014, respectively. Currently, he works at the Tokyo Gas Co., Ltd.

**Dag Heinemann** received his MSc degree in life science—cells and molecules at Leibniz University Hannover, Germany, in 2009. From 2009 to 2013, he passed on his PhD thesis concerning gold nanoparticle-mediated cell manipulation for biomedical approaches at Laser Zentrum Hannover e.V (LZH). Currently, he is the head of the Cytophonics Group of the LZH. His research interests include optical cell manipulation and transfection, optogenetics, and laser-based cell ablation.

**Alexander Heisterkamp** received his PhD and is an expert in biomedical optics, with a focus on nonlinear optics and the application of ultrashort laser pulses in medicine, especially nonlinear and linear imaging techniques, cell manipulation, and laser-tissue interaction. He holds a professorship for biophotonics at Leibniz University Hannover. He has been a member of SPIE for several years and is a SPIE fellow.

**Mitsuhiro Terakawa** received his BS, MS, and PhD degrees from Keio University in 2003, 2005, and 2007, respectively. In 2007, he joined the Wellman Center for Photomedicine, Massachusetts General Hospital, as a research fellow. He joined Keio University in 2009. Currently, he is an associate professor at Keio University. His research interests include ultrafast laser processing, laser processing of biomaterials, laser drug delivery, and laser-based nanostructure formation.